Computers and Electronics in Agriculture 194 (2022) 106735

Contents lists available at ScienceDirect

Computers and Electronics in Agriculture

journal homepage: www.elsevier.com/locate/compag

Developing and evaluating an autonomous agricultural all-terrain vehicle for field experimental rollover simulations

Hsiao-Yang Chou *, Farzaneh Khorsandi, Stavros G. Vougioukas, Fadi A. Fathallah

Department of Biological and Agricultural Engineering, University of California, Davis, United States

ARTICLE INFO

Keywords:
All-terrain vehicle
Autonomous
Crush protection device
Global positioning system
Rollover

ABSTRACT

Utility All-Terrain Vehicles (ATVs) are commonly used on farms for agricultural activities such as carrying implements, applying fertilizers, and transportation. Among all agricultural ATV incidents on farms, rollover crushes are the leading cause of fatalities. Crush Protection Devices (CPDs) are passive safety structures that potentially decrease the severity of injuries and the number of deaths in agricultural ATV rollover incidents. However, there are contradictions in the results of previous studies regarding the effectiveness of CPDs in protecting the operator in rollover incidents. The effectiveness of CPDs should be evaluated experimentally with an autonomous ATV, allowing repeatable and systematic rollover tests. This study aims at developing three automatic control systems on an ATV for future rollover simulations:

(1) Global Positioning System (GPS)- based navigation system that allows autonomous steering,
(2) remote cruise control module for keeping consistent riding speeds, and
(3) remote braking system for safety in future unmanned ATV tests.

The performance of each system was examined by operating the autonomous ATV in an outdoor testing terrain. The term autonomy in this study refers to the autonomous steering system, along with the remotely controlled speed and braking systems. Results showed that the developed systems performed within the acceptable range for conducting future rollover tests accurately and safely. Application of the autonomous ATV expects to deliver repeatable results in rollover simulations, and thus increases the reliability of CPD evaluation.

1. Introduction

All-terrain vehicles (ATVs) are off-road motorized vehicles that are widely used for occupational and recreational purposes. The ATV Safety Institute (ASI) (Helmkamp, 2012) reported more than 35 million individuals in the U.S. ride ATVs. According to an industry survey, 79% of ATV owners in the U.S. used the vehicle for recreation or sports and 21% used them for work or chores (General Accounting Office, 2010). Sport ATVs and utility ATVs have several design differences. Utility ATVs usually have front and rear racks for carrying loads, a trailer hitch for pulling implements, and winches for towing equipment; while most sport ATVs do not have the work-related attachments mentioned above. Moreover, most utility ATVs are four-wheel drive, and most sport ATVs are rear-wheel drive. These differences provide utility ATVs the ability to perform a wide range of tasks on farms, such as irrigation, towing equipment, animal round up, and other chores (Raphael Grzebieta et al., 2017b). This paper will focus on adult-sized utility ATVs that are used for agricultural activities.

Features of ATVs such as low-pressure tires, narrow wheelbase, narrow track width, and high center of gravity enhance their maneuverability (Ayers et al., 2018). However, these features make ATVs unstable, which can lead to fatal incidents. According to the Occupational Health and Safety Administration (OSHA), there were 2,090 ATV-related occupational injuries and 321 ATV-related fatalities occurred between 2003 and 2011, in which 60% of the occupational ATV fatalities occurred in the agricultural sector (Raphael Grzebieta et al.,

* Corresponding author at: One Shields Drive, 3038 Bainer Hall, Department of Biological and Agricultural Engineering, University of California, Davis, Davis, CA 95616, United States.
E-mail address: hchou@ucdavis.edu (H.-Y. Chou).

https://doi.org/10.1016/j.compag.2022.106735
Received 16 August 2021; Received in revised form 18 December 2021; Accepted 18 January 2022
Available online 4 February 2022

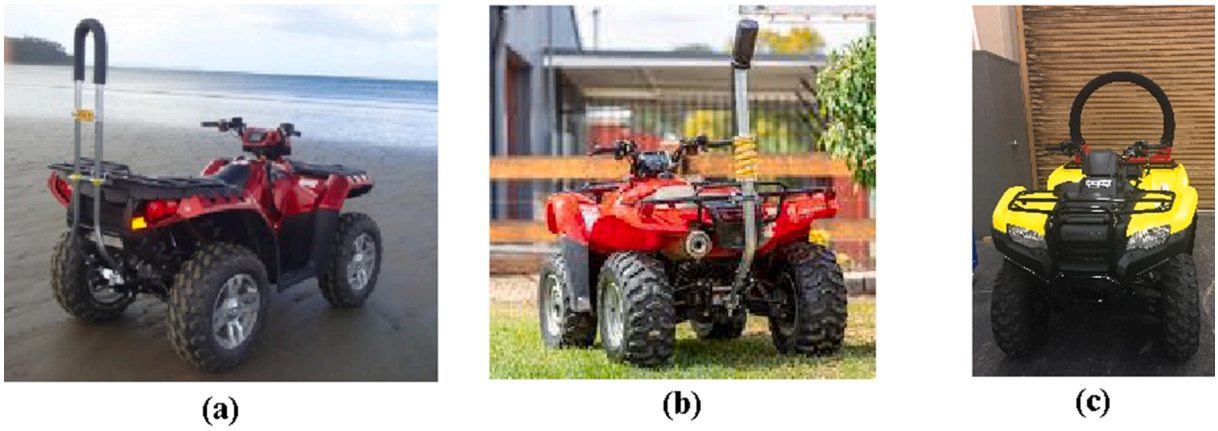

Fig. 1. Three CPD designs (a) Quadbar CPD (Helmkamp, 2012), (b) Quadbar Flexi CPD (Helmkamp, 2012), (c) Lifeguard CPD.

2017b). ATV rider may encounter rollover crashes or other incidents when traversing steep or uneven terrains (Raphael Grzebieta et al., 2017b). ATV not only has typically low rollover resistance, but also provides low margins of safety against rollover (Grzebieta et al., 2015b). Rollover crashes constitute 85% of fatal ATV incidents in the agricultural sector, with 68% of operators pinned under the ATV and 48% died as a result of mechanical asphyxiation (McIntosh et al., 2016).

1.1. Crush Protection Devices (CPD) evaluation

Passive safety structures such as Crush Protection Devices (CPD) have been developed to protect the ATV rider in rollover incidents. The adoption of these external structures prevents direct crushing and fatal compression on the rider by providing a crush protection zone (CPZ) under a rolled-over ATV (Khorsandi et al., 2019a,b). Several CPD models are commercially available, including Quadbar, Quadbar Flexi, and Lifeguard (Khorsandi et al., 2019a,b) (Fig. 1).

Multiple studies have shown that using CPD on ATVs reduces injuries in rollover crushes (Grzebieta and Achilles, 2007; Snook, 2009), and it reduces the chance of life-changing injuries by 70–80% (Lambert, 2011; Lower, 2013). Health and safety governmental agencies such as the National Institute of Occupational Safety and Health (NIOSH) also recommends installing CPDs (Helmkamp, 2012). Grzebieta et al. (2017a) reported that from the infield data, none of the rollover incidents involve CPDs had serious chest or head injury, which are the two main causes of death in ATV incidents, and the data suggested that CPDs prevented serious chest injuries in rollovers. However, up to this point, several studies have shown that CPDs have no statistically significant benefit in reducing injuries due to the possibility of it hitting the victim or restraining the operator from rapid separation from the ATV (Zellner et al., 2008). However, a survey showed that CPDs have protective benefit in rollover events, and the only reported case in which CPD caused injury to a rider was due to incorrect installation (Grzebieta et al., 2017a). Considering the inconsistent results from previous findings on whether CPDs prevented or caused injuries, further tests are needed to evaluate the performance of CPDs in ATV rollover incidents.

Several researchers experimentally evaluated the performance of CPDs with engineering control technologies (Khorsandi et al., 2021), using methods including static tests (Ridge, 2009; Sulman et al., 2007), dynamic stability and handling tests (Grzebieta et al., 2015a), and field-upset tests (Zellner and Kebschull, 2015). Static tests aimed to evaluate the structural strength and the deflection of a CPD in slow-motion deflection tests. Ridge (2009) conducted static tests based on standard ISO5700, which is a standard developed for Roll-over Protection Structure (ROPS) of small narrow tractors (International Organization for Standardization, 2013; Ridge, 2009). Standards of tractors may not be applicable for ATVs due to their significantly different structures and operational conditions. In addition, Sulman et al. (2007) applied the New Zealand Occupational Safety and Health Service's guideline (1998) in their static tests. The guideline was developed for ATV ROPS but had not been approved yet (Sulman et al., 2007).

For conducting the dynamic tests, researchers used either a tilted table or a vehicle accelerator to experimentally simulate ATV side rolls and backflips on downhill slopes (Grzebieta et al., 2015b). These tests aimed to evaluate the ATV motions, the stability, and the dynamic handling of ATVs with CPDs. However, dynamic tests conducted on a tilted surface had limitations on CPD evaluation. Due to technical difficulties in the testing setups, the slope length was often limited, and the surface conditions were not representative of actual field conditions. Thus, these studies for CPD evaluation are not adequate for testing CPDs in rollover incidents.

Researchers conducted field-upset tests to experimentally simulate rollover incidents (Zellner and Kebschull, 2015). The test includes low-speed turning on bumpy sloped surfaces and sharp turning in flat fields, which is called the J-turn test. Field-upset tests are preferred over both static and dynamic tests for evaluation of CPD performance since they provide a more realistic rollover simulation. However, the field-upset rollover tests performed in a previous study were controlled by the test engineers to drive the ATV to intended speeds and locations via a radio controller (RC), which is a barrier towards the replication of these tests (Zellner and Kebschull, 2015). There was limited evidence in the previous field-upset tests' results to be adequate to demonstrate the effectiveness of CPDs in ATV rollover incidents. Tests without automatic speed and steering systems were not repeatable due to human error (Zellner and Kebschull, 2015). Applying automatic control of speed, path, and overturn point for future ATV rollover tests and rollover simulations was recommended to improve test repeatability for injury mitigation purposes (Heydinger et al., 2016; Zellner and Kebschull, 2015).

Although these tests (static, dynamic, and field-upset tests) were informative regarding the performance of CPDs in ATV rollover incidents, they were not sufficient for proving the effectiveness of CPDs due to the limitations that were discussed in this section.

1.2. Objectives

The long-term goal of this study is to reduce the severity of injuries and the number of fatalities in agricultural ATV rollover crashes. Although CPDs can potentially protect the operator in ATV rollover incidents, there are contradictions among the results of previous studies regarding CPDs' effectiveness in protecting the operator in a rollover incident (Grzebieta and Achilles, 2007; Lambert, 2011; Lower, 2013; Snook, 2009; Zellner et al., 2008; Zellner and Kebschull, 2015; Zellner et al., 2013). Moreover, even though there are significant differences

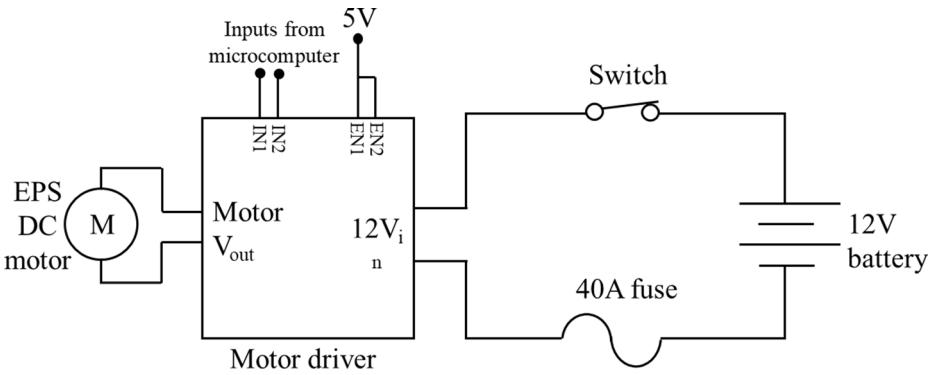

Fig. 2. EPS motor servo control circuit diagram.

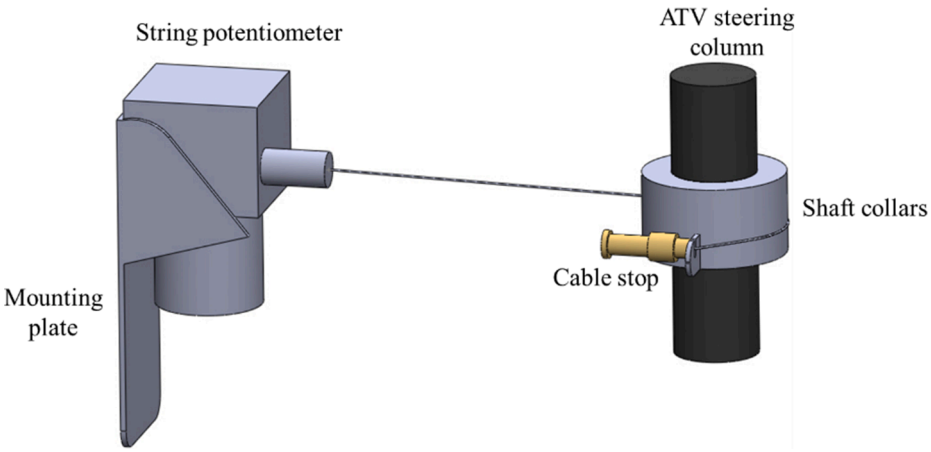

Fig. 3. 3D drawing of the feedback system (rear view).

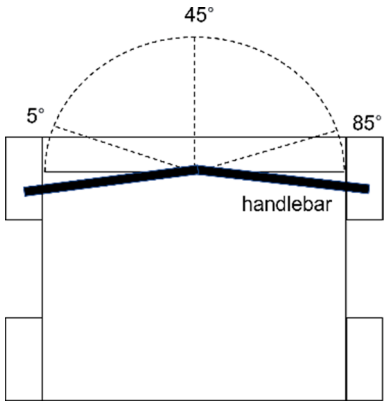

Fig. 4. ATV handlebar rotational degrees.

between agricultural and recreational ATV incidents, no study has evaluated specifically the performance of CPDs in agricultural ATV rollover incidents.

A hypothesis has been formulated based on previous studies that an autonomous ATV can reduce human error and deliver consistent results in future rollover simulations and CPD evaluations (Heydinger et al., 2016; Zellner and Kebschull, 2015). The overall goal of this study, which is a step towards the attainment of our long-term goal, is to develop an autonomous ATV for conducting repeatable and accurate unmanned ATV rollover simulations for evaluation of CPD performance in agricultural ATV incidents. This overall goal will be achieved through two specific objectives including:

1) **developing autonomous and remotely controlled systems on an ATV, and**
2) **evaluating the performance of autonomous and remotely controlled systems.**

Three control systems were developed to fulfill objective (1),

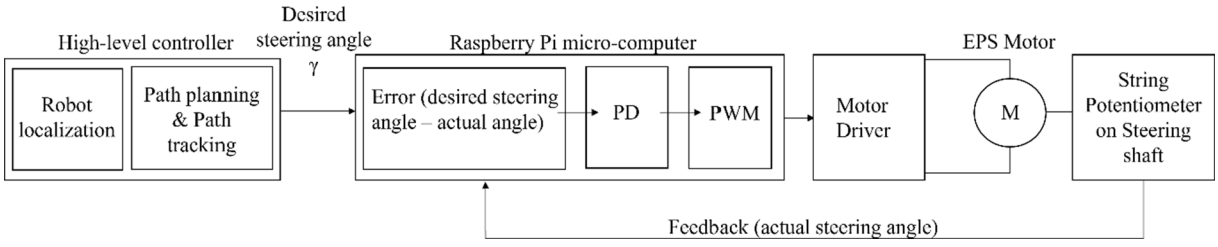

Fig. 5. An overview of the high-level controller and the low-level steering controller.

(a) (b)

Fig. 6. (a) GPS Base station installation on a tripod, (b) GPS Rover Station's antenna on ATV front rack.

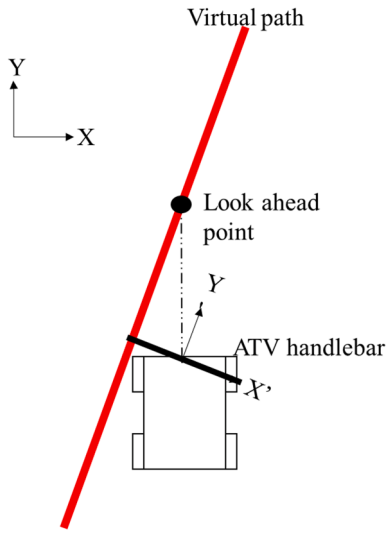

Fig. 7. The relative position and shift of ATV in world coordinates.

including the autonomous steering, the remote speed, and the remote braking systems. To fulfill objective (2), experimental riding tests were conducted to evaluate the performance of the three systems.

2. Materials and methods

2.1. Systems development

Autonomous systems were designed and developed on an ATV (2018 Honda 4x4 FourTrax Rancher, American Honda Motor Co., Inc., Torrance, CA). Three systems were developed, including: (1) steering control system with path-following navigation, (2) speed control system, and (3) remote braking system. In this paper, the word autonomy refers to the autonomous steering control system and the remotely controlled speed and braking systems. A remotely controlled system requires a human operator with a remote controller, such as a push-button or a joystick. In contrast, an autonomous system makes decisions based on computer programming and sensory feedback without human intervention.

The autonomous systems were specifically developed to conduct future unmanned ATV rollover tests; thus, the controllers developed in previous unmanned ATV studies should be adjusted to accommodate the following specific needs (Bascetta et al., 2009; Beainy and Commuri, 2009; Behringer et al., 2004; Heydinger et al., 2016; Rönnbäck and Johansson, 2011; Trebi-Ollennu and Dolan, 1999; Zellner and Kebschull, 2015). First, in future experimental tests, vehicle parts will be monitored in real-time to understand the pressure and impact forces on the ATV in a rollover incident. Therefore, the vehicle's overall shape and structure should be preserved. External devices outside of the ATV's existing structure, such as metal frames, stepper motors, and gears, should be avoided. Secondly, the ATV's handlebar is fragile and can be easily damaged in rollover tests; thus, we should avoid installing electronic components on the handlebar. Lastly, the manual drivability of the ATV should be maintained to allow normal ATV operations to ride the ATV between different test terrains.

2.1.1. Steering control system

The steering control system of the unmanned ATV aimed to provide repeatable and accurate line-following navigation. The system consisted of the low-level controller and the high-level controller. The low-level controller included a closed-loop motor control algorithm, which controlled the mechanical steering motion. The high-level controller included algorithms for robot localization, path planning, and path tracking. The algorithms calculated the desired steering angle (γ) based on the observed and intended position and orientation. An overview of the controllers is shown in Fig. 5.

2.1.1.1. Low-level servo controller. The low-level steering control system was developed using the vehicles' built-in electric power steering (EPS) unit. Many modern ATVs are equipped with an EPS unit, which is connected to the handlebar through a vertical steering column. The unit includes an EPS electric motor, an Electronic Control Unit (ECU), and a torque sensor. The EPS unit provides an additional assisting torque in the same direction as the driver's steering direction, which reduces the amount of steering torque required when turning the vehicle's steering handlebar. Controlling the EPS electric motor automatically can provide torque to rotate the ATV's steering column. Since ATVs' steering column and handlebar are connected, the steering mechanism can be mimicked as a rider is turning the handlebar. Using an EPS electric motor for automatic steering control also minimizes the change in the vehicle's shape and preserves the vehicle's manual drivability (Bascetta et al., 2009).

Since numerous input signals were taken into the EPS unit and the signals were difficult to duplicate (Cortner et al., 2012), the EPS motor was controlled separately with an additional low-level control system. A motor driver with a continuous current limit of 60 amps was used to drive the motor. A 40-amp fuse and a 100-amp switch were installed to

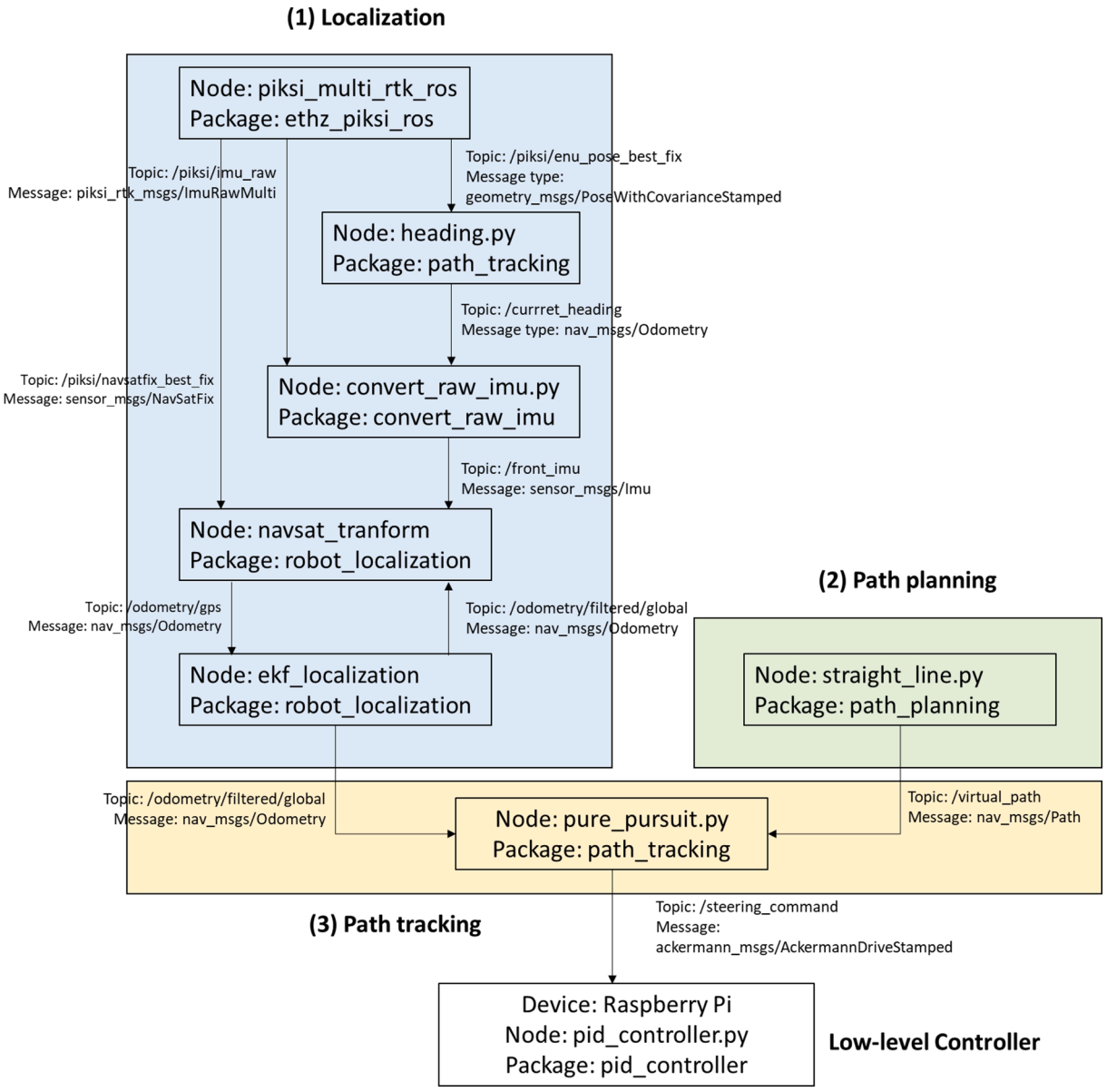

Fig. 8. The architecture of the high-level controller.

prevent over-loads. The circuit diagram of the low-level controller is shown in Fig. 2.

The low-level control system was developed using a Raspberry Pi single-board micro-computer (Model 4B, Raspberry Pi Limited, Cambridge, UK) with Linux operating system. Python was chosen to be the programming language of this application due to its wide variety in open-source modules to conduct the low-level controller.

Feedback signal of the closed-loop low-level system was provided from a draw-wire string potentiometer mounted near the ATV steering column using a shaft collar (Fig. 3). As the steering shaft rotated, rotational motion (in degrees) was transferred into linear motion (in meters), and then measured by the string potentiometer (in Voltage). Voltage outputs were sent to the Raspberry Pi through a 16-bit Analog-to-digital converter (ADC) chip. The feedback signal from the string potentiometer was calibrated to return the actual steering angle of the handlebar. The center of handlebar was defined as 45 degrees, with an increase of angles in the clockwise direction (Fig. 4).

The difference between the desired reference angle (γ) and the actual steering angle was calculated as an error, and the compensation output for such error was produced using the Proportional-Derivative (PD) controller. The Pulse-width Modulation (PWM) technique then created variable voltage level outputs from the PD controller's digital outputs. The PD controller and the PWM were implemented to calculate the processed signal for the motor driver, and then determine the rotational speed and position of the EPS electric motor (Fig. 5).

2.1.1.1.1. Low-level controller gains. The classical Proportional, Integral, Derivative (PID) controller calculation involves three constant gain parameters: proportional (P), integral (I), and derivative (D). The overall control function can be expressed mathematically as

$$u(t) = K_p e(t) + K_i \int_0^t e(t) + K_d \frac{de(t)}{dt}, \quad (1)$$

where u(t) indicates the weighted sum of the three terms and e(t) indicates the error value. In this study, the PID controller was tuned by adjusting the *P*, *I*, and *D* gains (K_p, K_i, and K_d) using the Ziegler-Nichols method (Ziegler and Nichols, 1942). The K_i, and K_d gains were first set to zero, then the K_p was increased until it reached a maximum value, at which the output started to oscillate. Finally, K_i, and K_d were tuned to account for any nonlinearities, such as backlash, friction, etc.

A preliminary test was conducted to determine the PID gains of the

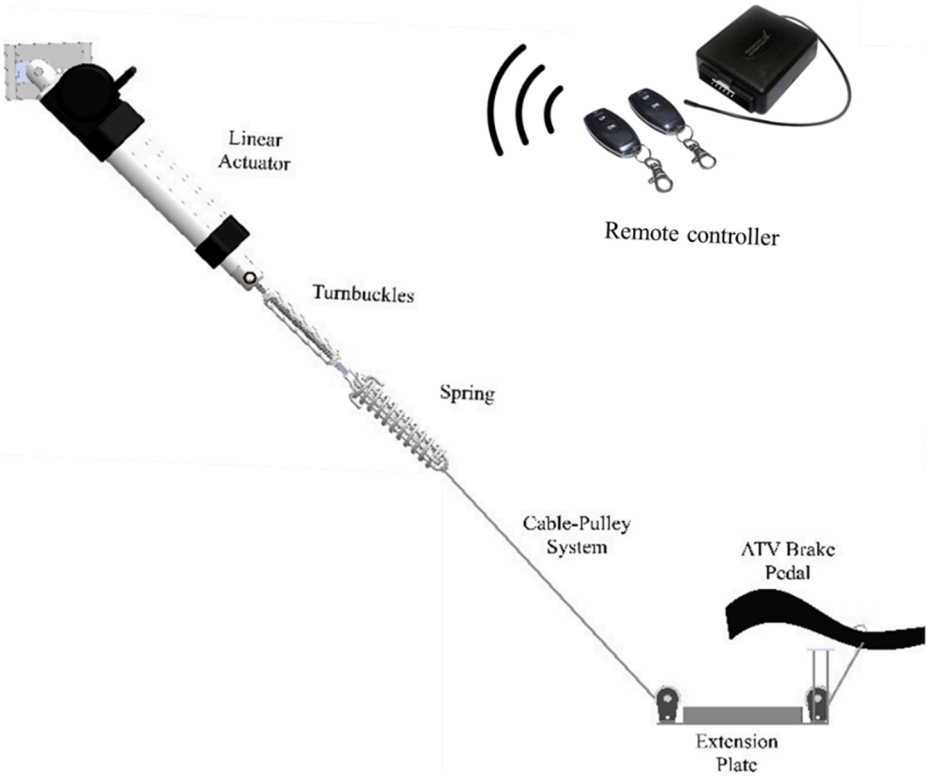

Fig. 9. SolidWorks drawing of brake system architecture.

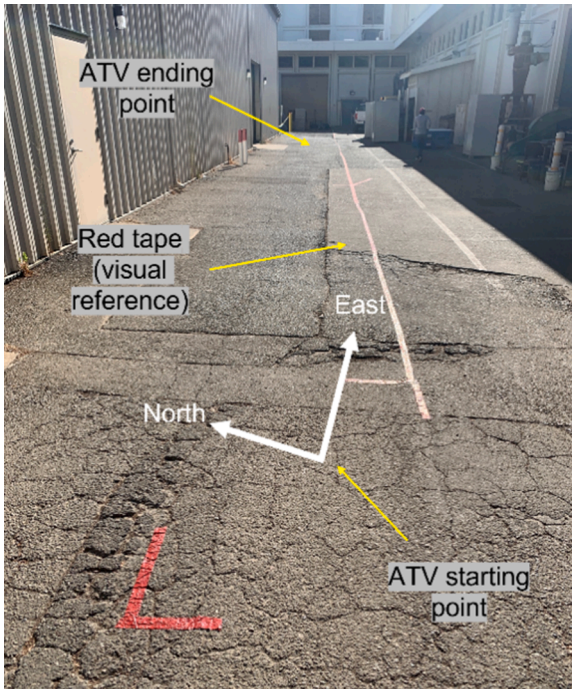

Fig. 10. ATV test terrain.

low-level controller. The ATV was first tested with its front-wheels lifted by a lift-jack, which significantly reduced the high friction between the ATV wheels and the ground surface. The ATV was then tested at a speed of 0.89 m/s (2 mph) with a rider. A pre-set reference angle of 45 degrees (center) was fed to the controller, and it was evaluated if the EPS electric motor could rotate the linkage of steering column and handlebar to the reference angle. The handlebar was manually rotated to extreme angles (5 and 85 degrees) to mimic the scenarios where the ATV was drifted. The gains of the PID controllers were selected as $K_p = 0.8$, $K_i = 0$, $K_d = 0.05$ when the ATV was statically lifted, and $K_p = 1.2$, $K_i = 0$, $K_d = 0.05$ when the ATV was in motion. Since the K_i gains were set to zero, we call it the PD controller in this paper. With these gains, the controller was able to reach the reference angle with minimum overshoots (<1 degree) and more smooth controller activity (less aggressive).

In order to avoid over-loading or over-heating the motor, the current draw of the EPS motor from the 12 V battery should be closely monitored. When the front wheels of ATV were lifted by a lift-jack, the friction between wheels and the ground was significantly reduced; thus, the EPS motor would draw approximately 5-10A. However, when the wheels were on the ground statically, the EPS motor would draw approximately 30-40A. Even with a 40-A fuse in the low-level steering system, a continuous large current should still be avoided to prevent damage to the battery and the motor driver. Thus, the autonomous steering system should not be operated statically.

2.1.1.2. High-level controller (Line-following Navigation). To deliver repeatable steering, the "line-following" method, which creates a predefined path that guides a robot, was adopted in this study. Global Positioning System (GPS) was selected to obtain the positional information due to its feasibility and accuracy in terms of satisfying the goal of this study: performing repeatable motion for rollover tests in an outdoor testing terrain. Most inexpensive GPS receivers have positional accuracy between 1.5 and 10 m, while Real-Time Kinematic (RTK) technology can make corrections to large errors and deliver centimeter-level accuracy. RTK technology uses a stationary "base station" to transmit the phase of GPS signal to the moving "rover", which then compares the received phase with the phase that they observed from satellites.

The high-level navigation includes three steps: (1) robot localization, (2) path planning, and (3) path tracking. Robot localization locates the position of ATV relative to a referenced coordinate system. The path planning algorithm creates a path for the ATV to follow. Lastly, the path

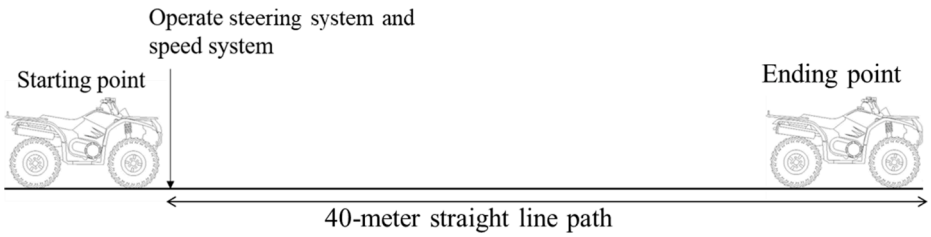

Fig. 11. Steering system test.

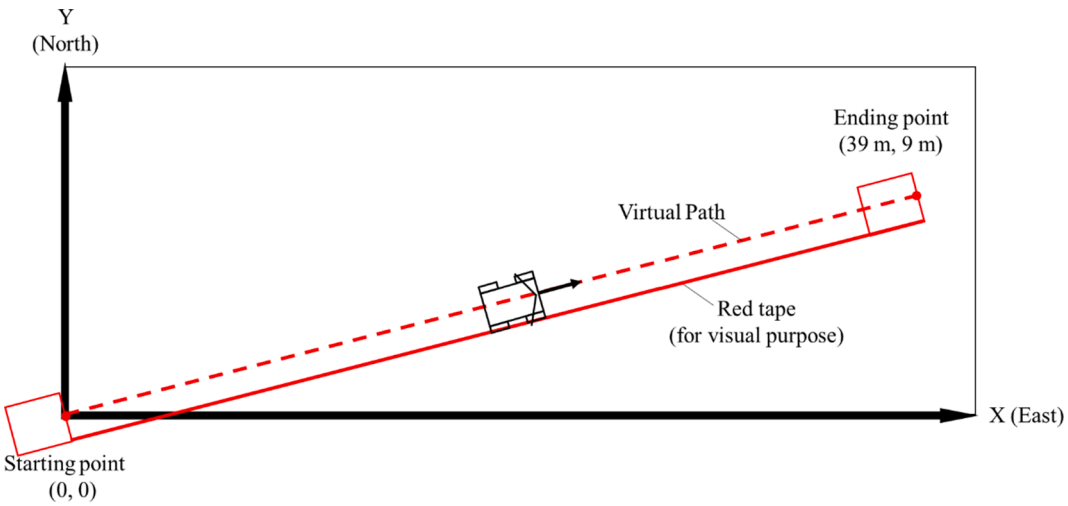

Fig. 12. ATV virtual path in the testing field.

Fig. 13. Ramp for ATV rollover tests.

tracking algorithm calculates the desired steering angle for the ATV to reach a location or follow the path with minimum error.

2.1.1.2.1. Robot localization. The GPS-based line-following system was developed using an RTK GPS module (Piksi Multi Evaluation, Swift Navigation, San Francisco, CA). The GPS antennas require an open sky-view for stable signals from satellites. Thus, the antenna of the base station was installed on top of a tripod to keep away from any obstructions to the sky-view (Fig. 6a). However, a tripod structure taller than the ATV handlebar would be vulnerable in rollover tests. Thus, the antenna of the rover station was installed on the ATV front rack, where the best sky-view could be observed, with an open-lid box that protected it from potential side impacts (Fig. 6b).

This GPS module was integrated within the Robot Operating System (ROS) (ROS Melodic, 2018, Open Robotics) on Ubuntu 18.04 server. ROS is a set of software libraries and tools that assists in robot development and applications. The ROS workspace and packages were installed and developed on a minicomputer (Intel Celeron N3350, AWOW) attached to the ATV.

An open-source package, *ethz_piksi_ros* (ETHZ ASL, 2019, ETH, Zurich, Switzerland), was installed in the ROS workspace. This package contained a Python ROS driver that supported the use of the Piksi Multi GPS module on the ROS platform. This driver has a "ROS node", *piksi_multi_rtk_ros* (Fig. 8), which is a process that performs computation, and then publishes (sends messages) or subscribes (receives messages) to ROS topics. This ROS node published multiple topics including (1) the GPS data (*/piksi/navsatfix_best_fix*) that contained the World Geodetic System (WGS84) coordinates in latitude, longitude, and altitude, and (2) the GPS data (*/piksi/enu_pose_best_fix*) that contains East-North-Up (ENU) coordinates in the local reference frame (x and y). The origin of the ENU coordinate can be defined by the user. In this study, the (0, 0) coordinate was defined as the starting location of the autonomous ATV's path.

The GPS measurements occurred intermittently, positioning at an update rate of 10 Hz, which was generally not desired because the system would become exposed to potential failures such as overshooting. To address this issue, an Inertial Measurement Unit (IMU) (BMI160, Bosch Sensortec, Dresden, Germany), with a higher update rate of 100 Hz, was implemented in the system, and the raw IMU data (*/piksi/imu_raw*) was published by the ROS node *piksi_multi_rtk_ros*. However, the IMU measurements were not blended with the GPS position or attitude solution. Moreover, an IMU alone would lead to a dead-reckoning system, which could lead to cumulative errors in distance estimates. To counteract these drawbacks, the navigation system used the Extended Kalman Filter (EKF) to produce the optimal estimation of states (vehicle's position and heading) by integrating two sensor data: GPS and IMU, into a combined position.

The software package *robot_localization* is a general-purpose state estimation package that was used to fuse multiple sensor measurements with the implementation of the EKF (Moore and Stouch, 2016). This

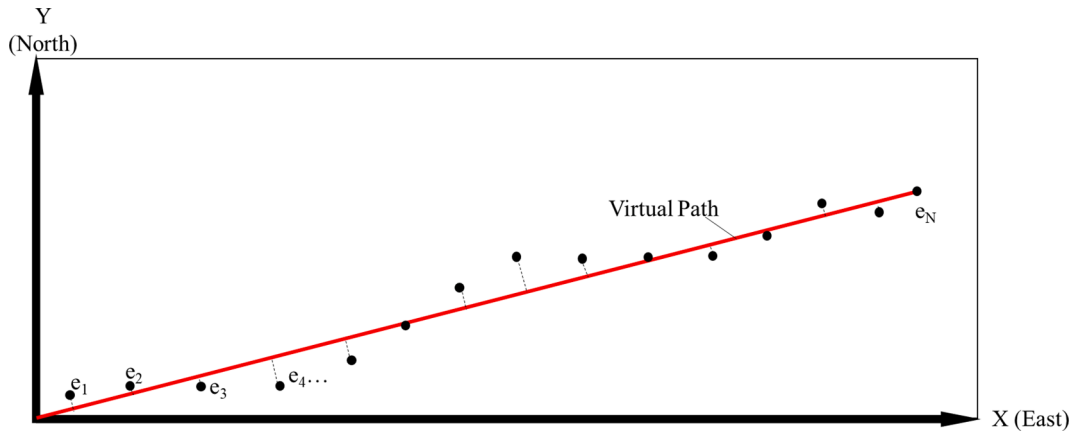

Fig. 14. Positional errors from the ATV trajectory to the virtual path.

Fig. 15. Speed system test.

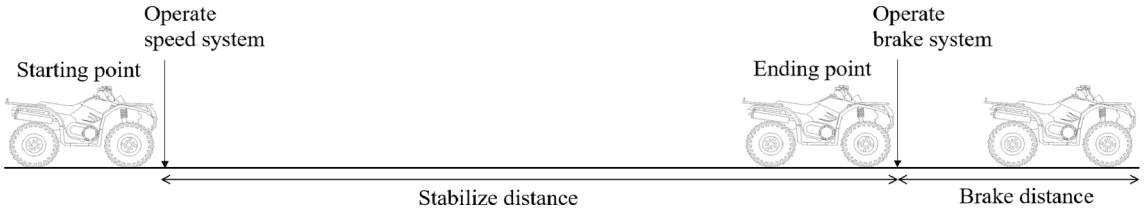

Fig. 16. Brake system test.

package provides continuous nonlinear state estimation of vehicle moving in 3D space; thus, it is largely used in vehicle or mobile robot navigation. There are two ROS nodes in the package: the sensor data pre-processing node "*navsat_tranform*" and the state estimation node "*ekf_localization*." The sensor data pre-processing node converted GPS's geodetic coordinates (latitude and longitude) into the local reference coordinates (ENU), and the state estimation node implemented the EKF. The raw IMU data (*/piksi/imu_raw*) published by Piksi Multi was not in a correct format to be fed into the *robot_localization* package. Thus, a ROS node "*convert_raw_imu*" was operated to provide the correct ROS message type (*sensor_msgs/Imu*), which adhered the ENU coordinates to be used in the *robot_localization* package.

In this study, a single GPS antenna and the IMU did not provide an absolute (earth-referenced) heading information. Therefore, the absolute heading was obtained from the updated GPS data using another ROS node "*heading*." This node obtained a most recent GPS data in ENU coordinate and compared with a previous GPS point to calculate the yaw value. An overall block diagram of the robot localization is shown in Fig. 8.

2.1.1.2.2. Path planning. The RTK GPS data of the initial and the goal positions in ENU coordinates were recorded in the field manually, where the straight line between the two positions was defined as the "virtual path." The path was constructed by calculating 100 intermediate points between the two inputted positions. The orientation of the path was calculated as the yaw between the starting and the ending ENU coordinates. A ROS node, "*path_planning*", was created to publish the path message (*/virtual_path*) to the path tracking controller. A block diagram of the path planning is shown in Fig. 8.

2.1.1.2.3. Path tracking. The pure pursuit algorithm is one of the widely used path tracking systems in the autonomous vehicle and robotic field. This algorithm computes the path curvature for a vehicle to maneuver from its current position to a "look-ahead point", which is a goal position on the path that is some distance ahead of the current position (Coulter, 1992). The "look-ahead distance" is the main tuning property, which determines how far the robot is "looking" from its current position to the look-ahead point (Fig. 7). A ROS node, *path_tracking*, contained a python file with the pure pursuit algorithm. The inputs of the *path_tracking* node were: (1) the EKF filtered output published by the *ekf_localization* node, and (2) the desired path's coordinates published by the *path_planning* node. The output of the *path_tracking* node was the steering angle (γ) of the vehicle, which was the input of the low-level controller discussed in Section 2.1.1.1. A standard ROS message developed for vehicles using front-wheel Ackermann steering (Ackermann Group, 2017), was used to publish the steering angle output. A block diagram of the path tracking is shown in Fig. 8.

2.1.2. Speed control system

The ATV speed is usually controlled with a thumb throttle lever on the handlebar. This lever gives ATV riders more flexibility compared to pedal accelerator, as it allows riders to shift their body weight for active

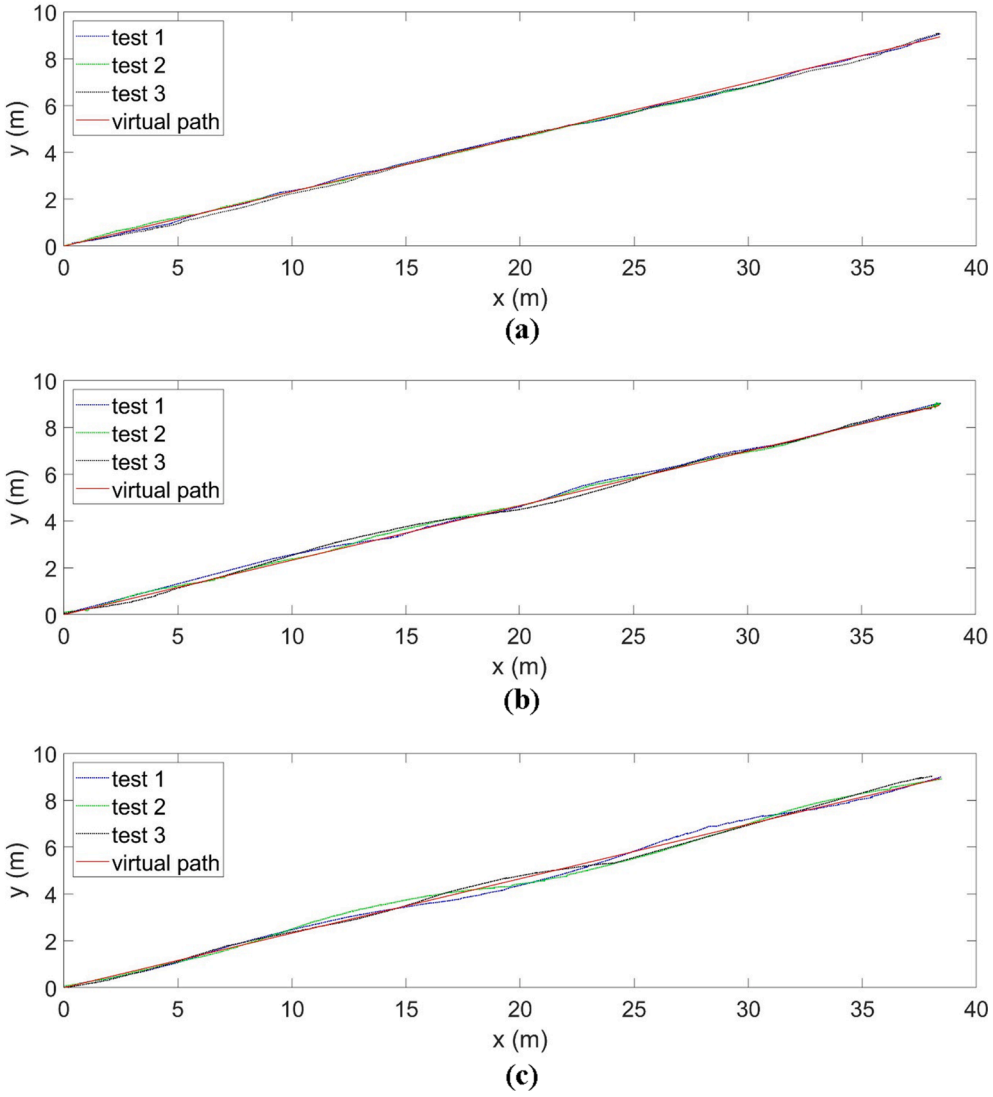

Fig. A1. (a) ATV trajectory at 2mph. (b) ATV trajectory at 5mph, (c) ATV trajectory at 10 mph.

riding and optimal vehicle maneuverability. In future rollover simulations, the ATV handlebar is one of the parts that will possibly hit the ground and be destroyed. Thus, additional installation on the handlebar, such as the throttle valve controller (Bascetta et al., 2009), should be avoided in this study. An ATV cruise control unit (MC S2580E, MCCruise, Mount Waverley, Australia) was selected since the system was covered and protected under the ATV structural frame; moreover, the system maintained the use of original throttle cable on the ATV to preserve the manual drivability. The control unit is a precise cruise control system consisting of a computer unit, electric throttle servo, Cable Interface Unit (CIU), and Bluetooth module for remote controls (MCCruise, 2018). The accuracy of the remote speed system is required to be high (within ± 2 mph of error) for repeatable results.

2.1.3. Emergency braking system

In addition to the steering control and speed control systems, safety precautions are needed to prevent out-of-control situations. Most ATVs include a foot brake pedal that is usually on the rider's right foot side and usually one or two hand brake levers on the ATV handlebar. In order to prevent potential damage on the handlebar, the remote braking system was designed and installed on the right foot brake pedal of the autonomous ATV. The remote braking system will be activated if the unmanned ATV is disoriented or goes over the intended speeds in future rollover tests.

Components of the remote braking system included a battery, a linear actuator (PA-04 IP66, Progressive Automations), a pulley-cable system, a remote controller (PA-31, Progressive Automations), and other mechanical mounts. A 3D representation and a picture of the braking system architecture are shown in Fig. 9.

The 2-inch stroke linear actuator has an actuation force of 100 lbs. The stroke length was chosen due to the limitation of ATV brake pedal displacement, which was approximately 1.5 in.. A 6-inch 100lbs/in extension spring was therefore installed to provide an extended length of approximately 0.5 to 1 in., which prevented an over-loading situation of the linear actuator motor. All components of the brake system had capacities greater than the 100-lbs limit.

The brake system was remotely controlled with a 12 V 20-amp motor controller box. The motor controller box was directly connected to the linear actuator motor. Under automatic operation, when the handheld remote was pressed, the actuator would retract and activate the brake. The handheld remote had a transmission range of 10 to 15 m in the open air. By pressing the handheld remote, the linear actuator should be activated instantly, and pulls down the brake pedal within 2 s.

A remote engine shut-off system or "kill-switch" (RES12VX, 3Built LLC, West Hills, CA), independent of the braking system, was installed on the unmanned ATV in case of the failure of the remote braking

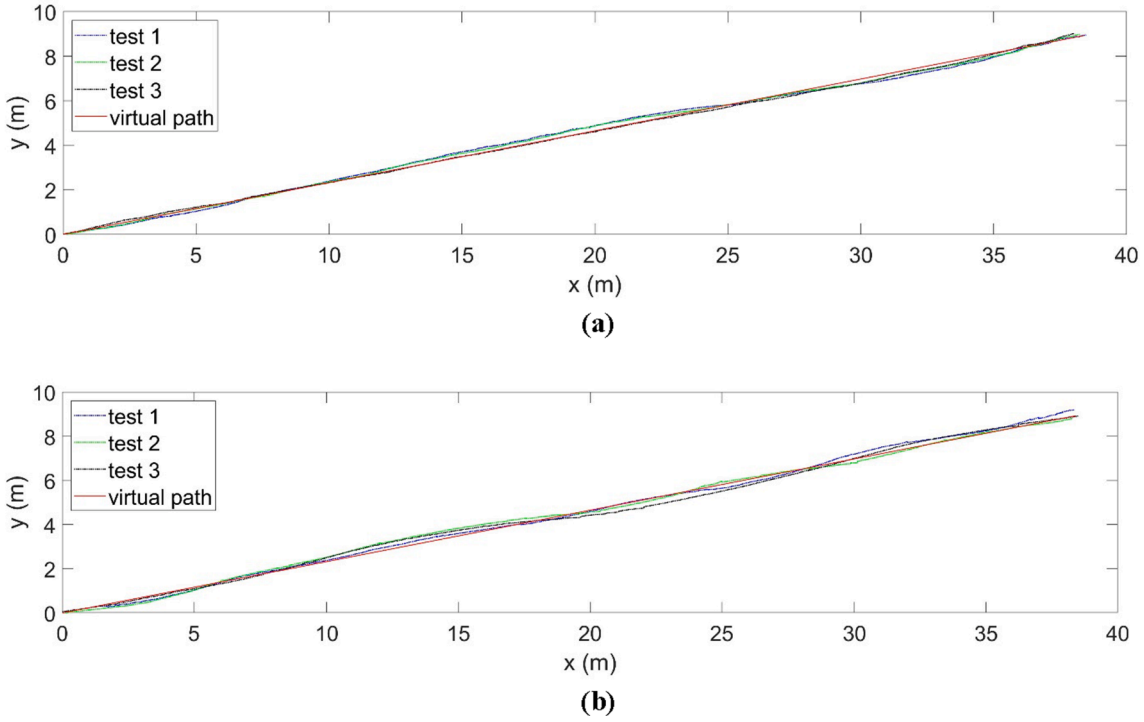

Fig. A2. (a) ATV trajectory at 2 mph with various loads, (b) ATV trajectory at 5 mph with various loads.

Table 1
Average deviations at various speeds.

Speed (m/s)	Average deviation of the three replications (m)	Standard Deviation
0.89	0.0623	0.00456
2.24	0.0704	0.0184
4.47	0.0654	0.0234

Table 2
ANOVA one factor test of speeds.

Source of Variation	*SS*	*df*	*MS*	*F*	*P-value*	*F crit*
Between Groups	0.003335	2	0.001667	2.727968	0.143669	5.143253
Within Groups	0.003667	6	0.000611			
Total	0.007002	8				

Table 3
Average deviations at various loads for speed of 0.89 and 2.24 m/s.

Speed (m/s)	loads (kg)	Average deviation (m)
0.89	0	0.107015
	63	0.142488
	91	0.06138
2.24	0	0.142488
	63	0.105757
	91	0.046419

system. The remote engine shut-off system aimed to terminate the unmanned ATV's acceleration via another handheld remote. The receiver module had an internal 10-amp relay and could receive signals from the handheld remote from up to 76.2 m in the open air. However, this alone was not sufficient to completely stop the vehicle in motion due to inertia, especially if the vehicle was operated on high speeds or steep slopes.

2.2. Evaluating the autonomous ATV performance

The performance of the autonomous ATV was evaluated to compare the autonomous and remote-controlled systems' compliance with their specified requirements for simulating rollover incidents. In experimental rollover tests, the autonomous ATV will be operated along a path and drive onto obstacles or ramps. Thus, the focus was on whether the autonomous ATV had the ability to reach an intended location with repeatable and accurate speeds. Since the autonomous ATV may also be used in other experiments such as dynamic handling tests and other driving tests, the ability of the autonomous ATV following the virtual line was also closely examined.

The maximum speed of the future rollover experiment is 6.7 m/s (15 mph). This speed is selected based on previous studies recommendation (Zellner and Kebschull, 2015). The speed control system of the autonomous ATV requires a terrain length of at least 27.35 m to reach such speed. An extra length is required to ensure sufficient brake distance. In this study, the test terrain for steering, speed, and braking system evaluations was a 40-meter straight, flat, non-smooth (with bumps and cracks) asphalt driveway between two buildings with an approximate width of 5-meter (Fig. 10). Due to safety concerns of operating the autonomous ATV on a narrow driveway, a rider was on the ATV during most tests. The rider would not intervene in the tests normal situations but would steer or brake on the ATV when it was off controlled.

Since a rider was on the autonomous ATV in this study, the maximum speeds of both the speed evaluation and braking evaluation were reduced from 6.7 m/s to 5.8 m/s due to safety concerns. As for the autonomous steering tests, the maximum speed was reduced to 4.47 m/s. If the steering system was off controlled under a high speed (5.8 or 6.7 m/s), the rider would not have enough time to stop the ATV, as the test terrain was narrow. In future rollover experiment, the autonomous ATV will be operated on a longer and larger terrain. Therefore, conducting the test with a maximum speed of 6.7 m/s on those terrains will be safe.

2.2.1. Steering system evaluation

The autonomous steering system was evaluated on an approximate 40-meter straight-line path with a three-inch wide red tape stick to the

Table 4
ANOVA two-way test of two speeds and three loads.

Source of Variation	*SS*	*df*	*MS*	*F*	*P-value*	*F crit*
Sample (speeds)	2.60E-05	1	2.60E-05	0.017844	0.898101	5.987378
Columns (loads)	0.002278	2	0.001139	0.78033	0.499775	5.143253
Interaction	0.001622	2	0.000811	0.555698	0.600605	5.143253
Within	0.008759	6	0.00146			
Total	0.012686	11				

Table 5
Average stabilized distance for speeds of 2.24, 4.47, 5.8 m/s.

Speed (m/s)	Average stabilized distance (m)	Standard Deviation	Coefficient of Variation
2.24	7.118	0.738	0.104
4.47	15.415	1.0871	0.0705
5.8	24.134	1.0977	0.0455

Table 6
ANOVA one factor test of stabilized distances at three levels of speeds.

Source of Variation	*SS*	*df*	*MS*	*F*	*P-value*	*F crit*
Between Groups	645.1626	2	322.5813	337.2421	1.35E-10	3.982298
Within Groups	10.5218	11	0.956527			
Total	655.6844	13				

Table 7
Average stabilized time for speeds of 2.24, 4.47, 5.8 m/s.

Speed (m/s)	Average stabilized time (s)	Standard Deviation	Coefficient of Variation
2.24	4.7	0.707	0.15
4.47	6.32	0.295	0.0467
5.8	7.85	0.777	0.099

Table 8
ANOVA one factor test of stabilized times at three levels of speeds.

Source of Variation	*SS*	*df*	*MS*	*F*	*P-value*	*F crit*
Between Groups	22.20557	2	11.10279	29.37245	3.88E-05	3.982298
Within Groups	4.158	11	0.378			
Total	26.36357	13				

Table 9
Average brake distances for speeds of 2.24, 4.47, 5.8 m/s.

Speed (m/s)	Average brake distance (m)	Standard Deviation	Coefficient of Variation
2.24	5.827	0.413	0.0709
4.47	11.770	0.577	0.049
5.8	16.220	0.574	0.0354

Table 10
ANOVA one factor test of brake distances at three levels of speeds.

Source of Variation	*SS*	*df*	*MS*	*F*	*P-value*	*F crit*
Between Groups	271.9303	2	135.9651	489.5766	3.15E-12	3.885294
Within Groups	3.332638	12	0.27772			
Total	275.2629	14				

ground for visual purposes. The "starting point" (the beginning of the 40-meter path) and the "ending point" (the end of the 40-meter path) of the ATV were manually marked on the terrain (Fig. 11).

The positional data of the autonomous ATV could be obtained with the RTK GPS module of the steering control system, which provided the GPS coordinates in the geodetic frame (latitude, longitudes, and altitude). The GPS coordinates at the starting point and the ending point were recorded and inputted in the GPS-based navigation system. The starting point was set to be the "origin" of the local reference frame (ENU) (Fig. 12).

Since the absolute heading (yaw) of the ATV was obtained from two ENU coordinates (Section 2.1.1.2.1), the ATV was required to start from a small distance behind the starting point to receive an "initial heading." The ATV was started approximately 2 m behind the starting point before the steering system was started. After an initial heading was recorded, the remote speed system and the steering system were activated at the starting point.

The ENU coordinates of the ATV throughout the travel were collected in each steering test. The performance of the steering system was evaluated by comparing the ATV's travel coordinates with the virtual path's ENU coordinates. The allowable positional error of the autonomous steering system is within ±20 cm at the ending point. This ±20 cm allowable error was determined from the width of a ramp in the side-upset rollover test (approximately 76 cm) (Fig. 13) and the width of ATV tires (approximately 20–25 cm). In rollover tests, one side of the ATV (two wheels on the same side) will drive up onto the ramp in order to create a tilting scenario.

Two sets of tests were conducted to evaluate the autonomous steering system: (1) steering at various riding speeds, and (2) steering with

Table 11
Average brake times for speeds of 2.24, 4.47, 5.8 m/s.

Speed (m/s)	Average brake time (s)	Standard Deviation	Coefficient of Variation
2.24	2.668	0.445	0.167
4.47	3.429	0.124	0.036
5.8	3.939	0.182	0.046

Table 12
ANOVA one factor test of brake times at three levels of speeds.

Source of Variation	*SS*	*df*	*MS*	*F*	*P-value*	*F crit*
Between Groups	4.093913	2	2.046956	24.8799	5.38E-05	3.885294
Within Groups	0.987282	12	0.082274			
Total	5.081195	14				

various loads on the ATV.

2.2.1.1. Steering at various riding speeds. A study was conducted to evaluate the effect of vehicle speeds on the ATV's steering performance. Three riding speeds were selected for this study: 0.89, 2.24, and 4.47 m/s. A total of nine tests were performed, where each speed test was conducted with three replications in a completely randomized order. A 91 kg rider rode the ATV for these tests. In this experiment, the dependent variable was the average deviation (positional errors in meters, e_i) from the ATV to the virtual path (Fig. 14). The average deviation was calculated as

$$Average\ \ deviation = \frac{|e_1|+|e_2|+\cdots+|e_N|}{N} \quad (2)$$

The ANOVA model (one-factor) tests were performed to evaluate the effectiveness of three levels of speeds on the dependent variable (average deviations). The fixed effects were the speed parameters. All statistical analyses were performed at an alpha level of 0.05.

2.2.1.2. Steering with various loads on the ATV. In future rollover tests, an anthropometric test device (ATD) Hybrid-III frontal impact dummy will be used to mimic a rider on the ATV. Since the weight of the riders in this study was different from the selected ATD (95th percentile male ATD is 101 kg, 50th percentile male ATD is 78 kg), a study was conducted to evaluate the effect of rider weight on the dependent variable (average deviations). The autonomous ATV was tested at various loads: (1) a 91 kg rider on ATV, (2) a 63 kg rider on ATV, and (3) ATV without a rider (0 kg). Six tests were performed in a completely randomized order, where the three levels of loads (0, 63, and 91 kg) were tested at speeds of 0.89 and 2.24 m/s. The testing speed of 4.47 m/s was eliminated due to safety concerns of having no rider on an autonomous ATV. In this experiment, the response variable was the average deviation from the ATV to the virtual path. The two-way ANOVA tests were performed to evaluate the effectiveness of fixed effects (three levels of loads and two levels of speeds) on the dependent variable (average deviations).

2.2.2. Speed system evaluation

The speed system on the autonomous ATV was evaluated with three levels of speeds, including 2.24, 4.47, 5.8 m/s (5, 10, and 13 mph) with a rider on the ATV. Five replications were conducted for each riding speed. The position where the speed system was operated defined the "starting point", and the position where the ATV reached the desired speed defined the "ending point" (Fig. 15). The "stabilize distance" and "stabilized time" were defined as the distance and the time of ATV traveled between the starting and the ending point, respectively. The velocity and ATV's position were acquired using the GPS system on the ATV and evaluated after the experiments. The average stabilized distance and stabilized time of the five replications were the dependent variables and were measured for all three riding speeds on the same testing terrain. Two single-factor ANOVA tests were performed to evaluate whether the speeds had a significant effect on the stabilized distances and times.

2.2.3. Emergency braking system evaluation

The braking system was evaluated at three speed levels of 2.24, 4.47, 5.8 m/s with a rider operating the ATV. Five replications were conducted for each riding speed. The remote speed system was activated at the "starting point." The remote braking system was activated when the ATV had reached and stabilized at the speeds at the "ending point" (Fig. 16). After the ATV has fully stopped, the distance between the ending point and where the ATV was fully stopped was measured, which was called the "brake distance." The time needed for ATV to completely stop from the ending point was called the "brake time."

In order to reduce the effect of human error, a high-speed camera (Chronos 1.4 Color High-Speed Camera, Krontech, Burnaby, BC, Canada) was used to take slow-motion videos at 1,502 frames per second. The slow-motion videos were used to examine the brake distance and the brake time, which were the dependent variables. In future rollover simulations, for the safety of unmanned ATV operation, the allowable brake time is within five seconds for all tested speeds, and a maximum of 20 m of brake distance. A single factor ANOVA test was performed to evaluate whether the speeds had a significant effect on the brake distances and times.

3. Results

The results of evaluating the steering control system, the speed control system, and the remote braking system are presented in this section.

3.1. Steering system performance

In this section, the performance of the autonomous steering system was evaluated by conducting two tests: (1) steering at three riding speeds, and (2) steering with three different loads on the ATV.

3.1.1. Steering system at various speeds

The trajectories of the autonomous ATV for three levels of speed are shown in Appendix A (Fig. A.1). Overshooting can be observed in those trajectories with higher levels of speeds (2.24 and 4.47 m/s), which made the ATV deviated from the desired path during the line following task. However, the accuracy of reaching the ending position is more essential to the experimental rollover simulation; therefore, the positional errors at the ending point were further evaluated. The average ATV ending positional errors were 15 cm, 7 cm, and 8 cm under the speeds of 0.89, 2.24, and 4.47 m/s, respectively. These errors are within the acceptable range of ±20 cm for future experimental ATV rollover tests (Section 2.2.1).

The ending positional error for the 0.89 m/s speed level was the greatest among other speed levels (2.24, and 4.47 m/s). This could be due to a visible bump at the end of the path. When the ATV was operated under slow speed (0.89 m/s), the ATV did not have enough momentum to reach the ending point, and therefore stopped before the intended location. In future rollover tests, such limitations in the testing terrain will be avoided. Thus, the data was again evaluated after eliminating the last 1-meter positional data from all tests at 0.89, 2.24, and 4.47 m/s. The average deviation of the entire trajectory (Fig. 14) was calculated for each steering test, and the average deviation of the three replications at each speed is shown in Appendix B (Table 1). There was no statistically significant difference between the average deviations at various speeds of 0.89, 2.24, and 4.47 m/s ($p = 0.144$).

3.1.2. Steering system with various loads

The statistical analysis showed that both riding speeds and the amount of load added do not have a significant effect on the steering system's performance ($p = 0.898$ and 0.5, respectively). The interaction effect was not significant ($p = 0.6$) (Appendix B Table 3). The trajectories of the autonomous ATV with various loads are shown in Appendix A (Fig. A.2).

3.2. Evaluating the speed system performance

The stabilized times and distances were measured and reported for each speed (Appendix B Table 5 and Table 7). The performance of the speed system was repeatable, with the coefficient of variation of stabilized distance and stabilized time being<0.15 at all speeds. There is a linear relationship between the stabilized distances and speeds with an R-squared value of 0.9753. Moreover, the stabilized times and speeds has linear relationship with an R-squared value of 0.984. Results showed that by increasing the speed, the stabilized distance and stabilized time increased significantly ($p < 0.05$).

The predicted stabilized distance and time at a speed of 6.7 m/s are 27.35 m and 8.48 s. Thus, a conclusion can be made that the autonomous ATV will be able to reach and stabilize at the desired speeds at the ending point. In future rollover test, with an intended speed of 6.7 m/s, the stabilized distance and time will be considered for designing the future field upset test terrain.

3.3. Emergency braking system performance

The average brake distances and brake times of the remote brake system were measured and reported for each speed (Appendix B Table 9 and Table 11). The performance of the brake system was shown to be repeatable with the coefficient of variation of average brake distance and brake time being<0.167 for all speeds. The brake distance and time were within the allowable error of 20-meter brake distance and 5-second brake time under speeds of 5.8 m/s.

The average brake distances and speeds have a linear relationship with an R-square value of 0.996; the average brake times and speeds also have a linear relationship with R-square of 0.999. Results showed that by increasing the speed, the brake distance and brake time increased significantly ($p < 0.05$).

The predicted brake distance and time at the speed of 6.7 m/s are 18.58 m and 4.24 s. In future rollover test, the brake time will be within the acceptable range of five seconds and 20 m. These findings will be applied to the design of future test terrain.

4. Discussion

The steering system performed well at speeds under 4.47 m/s with an acceptable positional error within the range of ± 20 cm, when no interruption was introduced. Statistical analysis showed that different speeds or loads (rider's weight) on the ATV did not have a significant effect on the steering system performance. However, additional tests are required to evaluate its performance at the intended speed of 6.7 m/s in future rollover tests, where a larger terrain will be used.

Our study demonstrated the repeatability and accuracy of the speed control system. Even though the stabilized distances would increase with increasing speeds, the predicted stabilized distance (27.35 m) at a future test speed of 6.7 m/s is within the range of the testing terrain. Thus, the autonomous ATV can stabilize at the intended speed in experimental rollover tests.

The emergency braking systems could stop the autonomous ATV remotely when needed. The predicted brake distance and time are 18.58 m and 4.24 s at the test speed of 6.7 m/s. Thus, we should consider approximately 20 m of allowable brake distance around the path when designing the field upset test terrain for future unmanned tests.

5. Conclusions

In this study, we developed and evaluated the performance of three control systems, including the autonomous steering, remote speed, and remote braking of the autonomous ATV. The developed autonomous ATV can accurately and precisely follow a path and reach an intended location with a consistent speed. In addition to reproducing the experimental rollover simulations, it can also be applied in other experiments that require repeatable motion, such as circular driving tests, J-turn test, and bump obstacle perturbation tests (Khorsandi et al., 2021). Applying these autonomous systems, human errors in previous studies can be reduced (Heydinger et al., 2016; Zellner and Kebschull, 2015). Therefore, the performance of CPDs can be evaluated accurately and systematically.

CRediT authorship contribution statement

Hsiao-Yang Chou: Conceptualization, Methodology, Software, Investigation, Formal analysis, Visualization, Writing – original draft, Writing – review & editing. **Farzaneh Khorsandi:** Conceptualization, Resources, Investigation, Writing – review & editing, Funding acquisition. **Stavros G. Vougioukas:** Supervision, Writing – review & editing. **Fadi A. Fathallah:** Supervision, Writing – review & editing.

Declaration of Competing Interest

The authors declare that they have no known competing financial interests or personal relationships that could have appeared to influence the work reported in this paper.

Acknowledgements

The research was supported by a grant awarded by the UC Davis Western Center of Agricultural Health and Safety (WCAHS) and a grant awarded by the National Institute for Occupational Safety and Health (NIOSH) #2U54OH007550. The content is solely the responsibility of the authors and does not necessarily represent the official views of NIOSH.

The authors would like to acknowledge the support provided by Guilherme De Moura Araujo, Justin Ho, Tom Bell, Andy Cobb, and Jedediah Roach of the Department of Biological and Agricultural Engineering for their assistance at various stages of this study. A special thank you goes to Benjamin Gatten and Chen Peng for providing the path tracking (pure pursuit) code in the ROS system.

Appendix A

See Figs. A1 and A2.

Appendix B

See Tables 1–12.

References

Ayers, P., Conger, J.B., Comer, R., Troutt, P., 2018. Stability Analysis of Agricultural Off-Road Vehicles. J. Agric. Saf. Health 24 (3), 167–182. https://doi.org/10.13031/jash.12889.

Bascetta, L., Magnani, G., Rocco, P., Rossi, M., Zanchettin, A.M., 2009a. Teleoperated and Autonomous All Terrain Mobile Robot (TA-ATMR). B&R First Eur. Ind. Ethernet Award. 12.

Bascetta, L., Magnani, G., Rocco, P., Zanchettin, A.M., 2009b. Design and implementation of the low-level control system of an all-terrain mobile robot. Paper presented at the 2009 International Conference on Advanced Robotics.

Beainy, F., Commuri, S., 2009. Development of an autonomous atv for real-life surveillance operations. Paper presented at the 2009 17th Mediterranean Conference on Control and Automation.

Behringer, R., Sundareswaran, S., Gregory, B., Elsley, R., Addison, B., Guthmiller, W., et al., 2004. The DARPA grand challenge-development of an autonomous vehicle. IEEE Intelligent Vehicles Symposium.

Cortner, A., Conrad, J.M., BouSaba, N.A., 2012. Autonomous all-terrain vehicle steering. Paper presented at the 2012 Proceedings of IEEE Southeastcon.

Coulter, R.C., 1992. *Implementation of the pure pursuit path tracking algorithm*. Carnegie-Mellon UNIV Pittsburgh PA Robotics INST.

General Accounting Office, 2010. All-terrain vehicles: How they are used, crashes, and sales of adult-sized vehicles for children's use: DIANE Publishing.

Grzebieta, R., Achilles, T., 2007. Report on quad-bar in relation to ATV rollover crashworthiness. Submitted to Victorian Coroner Inquest into ATV Deaths, Department of Civil Engineering, Monash University, Victoria, Australia.

Grzebieta, R., Rechnitzer, G., Simmons, K., 2015a. Dynamic handling test results. Quad Bike Performance Project TARS Res. Report (2).

Grzebieta, R., Rechnitzer, G., Simmons, K., McIntosh, A., 2015b. Final Project Summary Report: Quad Bike Performance Project Test Results, Conclusions, and Recommendations. Transport & Road Safety (TARS)-University of New South Wales, Sydney, NSW.

Grzebieta, R., Boufous, S., Simmons, K., Hicks, D., Williamson, A., Rechnitzer, G., 2017a. Quad bike and OPD workplace safety survey report: results and conclusions.

Grzebieta, R., Rechnitzer, G., Simmons, K., Hicks, D., 2017b. Rollover Crashworthiness of Quad Bikes and Side by Side Vehicles: A Comparative Laboratory Testing Study. Paper presented at the IRCOBI Conf. Proc.

Helmkamp, J.C., 2012. ATV Safety Summit: Vehicle Roll-Over Protection - Roll-Over Protection (NIOSH).

Heydinger, G., Bixel, R., Yapp, J., Zagorski, S., Sidhu, A., Nowjack, J., et al., 2016. Vehicle characteristics measurements of all-terrain vehicles. SEA Vehicle Dynamics Division, Columbus OH. For Consumer Products Safety Commission contract HHSP I.

International Organization for Standardization, 2013. ISO 5700: Tractors for agriculture and forestry - Roll-over protective structures (ROPS) Static test method and acceptance conditions. Geneva Switzerland: International Organization for Standardization.

Khorsandi, F., Ayers, P.D., Fong, E.J., 2019a. Evaluation of Crush Protection Devices for agricultural All-Terrain Vehicles. Biosyst. Eng. 185, 161–173.

Khorsandi, F., Ayers, P., Fong, E., 2019b. Evaluation of the Crush Protection Zone of Three Crush Protection Devices. Paper presented at: 2019 ASABE Annual International Meeting.

Khorsandi, F., Ayers, P.D., Myers, M., Oesch, S., White, D.J., 2021. Engineering Control Technologies to Protect Operators iIn Agricultural All-Terrain Vehicle Rollover Incidents. J. Agric. Saf. Health.

Lambert, J., 2011. Version 4 of a paper reviewing: Quad bike design. Computer simulation of Quad bike incidents as reported in various papers and presentations by Dynamic Research Inc, Quad manufacturers cynicism in respect of safety; and Quad bike safety improvements.

Lower, T., 2013. Quad bike fatalities costly - but manufacturers fail to act. Australian Centre for Agricultural Health and Safety. Retrieved from http://sydney.edu.au/news/84.html?newsstoryid=11296.

MCCruise, 2018. SL Honda TRX420 from 2014. Retrieved from https://www.mccruise.com/collections/honda-sl/products/sl-honda-trx420-500-from-2014?variant=49491956804.

Mcintosh, A.S., Patton, D.A., Rechnitzer, G., Grzebieta, R., 2016. Injury mechanisms in fatal Australian quad bike incidents. Traffic Inj. Prev. 17 (4), 386–390.

Moore, T., Stouch, D., 2016. A generalized extended kalman filter implementation for the robot operating system. In: Intelligent Autonomous Systems, vol. 13. Springer, pp. 335–348.

New Zealand occupational safety and health service, 1998. Guidelines for the Design, Construction and Installation of Rollover Protective Structures (ROPS) for All Terrain Vehicles. In. Wellington, New Zealand: Occupational Safety and Health Service, Department of Labour.

Ridge, C.J., 2009. QB Industries: Quad Bar Tests Model 401. Ridge Solutions, Dry Creek, South Australia.

Rönnbäck, S., Johansson, L., 2011. Field tests of a roll-over prevention system for quad-bikes. Paper presented at the 2011 IEEE International Conference on Mechatronics.

Snook , C. , 2009 . An assessment of passive roll over protection for Quad Bikes. Faculty of Engineering & Surveying Technical Reports. Report TR-2009-CS04 . University of Southern Queensland, Faculty of Engineering and Surveying , Queensland, Australia.

Sulman, R., Kapke, P., Robertson, D., 2007. Test report - ATV rollover protection structure, Sulman Forensics, Toowoomba, Queensland, Australia.

Trebi-Ollennu, A., Dolan, J.M., 1999. An autonomous ground vehicle for distributed surveillance: cyberscout.

Zellner, J., Van Auken, R., Kebschull, S., Munoz, S., 2008. Injury risk–benefit analysis of rollover protection systems (ROPS) for all-terrain vehicles (ATVS) using computer simulation, full-scale testing and ISO 13232. Paper presented at the Poster Presentation F2008-08-009, Fisita World Automotive Congress.

Zellner, J.W., Kebschull, S.A., 2015. Full-Scale Dynamic Overturn Tests of An ATV With and Without A “Quadbar” CPD Using an Injury-Monitoring Dummy. Dynamic Research Institute, Torrance, California.

Zellner, J.W., Kebschull, S.A., Van Auken, R.M., 2013. Evaluation of injury risks and benefits of a crush protection device (CPD) for all-terrain vehicles (ATVs). SAE Int. J. Passenger Cars-Electron. Electrical Syst. 7 (2013-32-9173), 41–72.

Ziegler, J.G., Nichols, N.B., 1942. Optimum settings for automatic controllers. Trans. ASME 64 (11).